Dense plasma diagnostics by fast proton beams

A. Golubev, M. Basko, A. Fertman, A. Kozodaev, N. Mesheryakov, B. Sharkov, and A. Vishnevskiy
Institute for Theoretical and Experimental Physics, Bolshaja Cheremushkinskaya 25, 117259 Moscow, Russia

V. Fortov, M. Kulish, V. Gryaznov, and V. Mintsev
Institute of Chemical Physics RAS in Chernogolovka, Chernogolovka, 142432 Moscow Region, Russia

E. Golubev, A. Pukhov, and V. Smirnov
State Optical Institute, Birjevaya liniya 12, 199034 St. Petersburg, Russia

U. Funk, S. Stoewe, and M. Stetter
Gesellschaft für Schwerionenforschung, D-64220 Darmstadt, Germany

H.-P. Flierl, D. H. H. Hoffmann, and J. Jacoby
Physikalisches Institut Universität Erlangen-Nürnberg, Erwin-Rommel-Strasse 1, D-91058 Erlangen, Germany

I. Iosilevski
Moscow Institute of Physics and Technology, Moscow, Russia
(Received 25 April 1997)

Coulomb energy losses by 3-MeV protons in a capillary discharge channel are used as a diagnostics tool to measure the plasma density. By combining the proton energy loss data with the electron temperature measurements,we have been able to diagnose the free electron density $n_{fe}=6.4\times10^{19}$ cm^{-3} in a 3.3-eV CH_2 plasma to an accuracy of $\pm17\%$. A considerably better accuracy can be expected for higher values of the electron temperature. [S1063-651X(98)08101-X]

PACS number(s): 52.40.Mj, 34.50.Bw

I. INTRODUCTION

Investigation of the interaction processes of ion beams with dense plasmas is one of the key issues in the physics of inertial confinement fusion driven by heavy ion beams [1,2]. This has motivated a series of experiments for measuring the effects of thermal ionization of the target material on the Coulomb stopping power for fast ions [3–7]. It was found that, in general, the stopping power is increased due to a combined effect of two mechanisms, namely because the effective charge of a projectile becomes higher and because the value of the Coulomb logarithm is increased. In particular, experiments of this type require reliable measurements of the plasma density in wide ranges of both the number density, $n_e\gtrsim10^{17}$–10^{19} cm^{-3}, and the areal density, $\int n_e\,dl\gtrsim10^{19}$–$10^{21}$ cm^{-2}, of the free electrons.

For relatively low plasma densities, several methods of plasma diagnostics, such as laser interferometry [8,9], laser light absobtion [10], Thomson scattering [11], and spectroscopic measurements [11,12], have been successfully applied. Unfortunately, for all of them there are physical reasons which prevent their application beyond plasma areal densities of $\simeq10^{21}$ cm^{-2} [11], mainly because the optical depth of the plasma volume becomes excessively high.

In this work we make an attempt to look at the problem of ion stopping from the other side, and employ the Coulomb energy losses as a method of plasma density diagnostics. It is well known that the Bohr-Bethe formula describes the Coulomb stopping power of cold matter to an accuracy of $\simeq1\%$ over a wide range of projectile energies [13]. The problem becomes especially clean and simple for protons, for which no complication due to the effective charge arises: so long as the velocity of a fast proton $v_p\gg e^2/\hbar=2.19\times10^8$ cm/s, its effective charge $Z_{eff}=1$. The idea is to invoke the plasma analog of the Bethe formula, i.e., the Larkin formula [14] (which must be no less accurate), to infer the areal density of the free electrons in a plasma from the measured values of the energy loss by fast protons. This method appears as particularly promising for the case of hot and dense ($n_e\gtrsim10^{19}$ cm^{-3}) plasmas, where most of the other techniques fail. The main objective of this paper is to demonstrate the possibilities of fast proton beams as a potential tool for dense plasma diagnostics.

II. THEORETICAL BACKGROUND

The diagnostics method that we explore here is based on the formula

$$\frac{dE_p}{dx}=-\frac{4\pi e^4}{m_e v_p^2}n_{fe}L_{fe},\quad L_{fe}=\ln\frac{2m_e v_p^2}{\hbar\omega_p},\tag{1}$$

which describes the stopping power of free electrons for fast protons in a plasma [14]. Here v_p and E_p are, respectively, the velocity and the kinetic energy of fast protons in a probe beam, n_{fe} is the number density of free electrons in a target, $\omega_p=(4\pi n_{fe}e^2/m_e)^{1/2}$ is the plasma frequency, and m_e and $-e$ are, respectively, the electron mass and its electric charge.

A remarkable feature of Eq. (1) is that, provided that E_p is known, it contains only one unknown quantity, i.e., the density of free electrons $n_{\rm fe}$. Equation (1) is applicable when (i) the proton velocity v_p is much higher than the thermal velocity of free electrons $v_e=(2T_e/m_e)^{1/2}$, and (ii) the quantum limit $\hbar v_p \gg e^2$ is realized for the Coulomb scattering of free electrons by a fast proton. One readily verifies that both these conditions are satisfied in our experiment described below, where $E_p=3$ MeV and $T_e \simeq 3.3$ eV.

Assume for a moment that a probe beam of fast protons propagates through a uniform column of length l of a fully ionized plasma. Having measured the proton energies at the entrance, E_{p0}, and upon the exit, E_{p1}, from the plasma column, one readily infers the value of $n_{\rm fe}$ by solving the equation

$$n_{\rm fe} l = \frac{E_{p0}^2 - E_{p1}^2}{4\pi e^4 L_{\rm fe}} \frac{m_e}{m_p}, \tag{2}$$

which is obtained from Eq. (1) in the nonrelativistic case, when $E_p = \frac{1}{2} m_p v_p^2$, under the assumption that the Coulomb logarithm $L_{\rm fe}$ remains constant over the energy interval $E_{p1} < E_p < E_{p0}$ (the latter is well satisfied in our case).

Since Eq. (1) is the key element of the diagnostic method under discussion, a few comments on its validity would be in order. Theoretically, Eq. (1) can be considered as firmly established, at least for the case when $L_{\rm fe} \gg 1$ and the plasma is weakly coupled [14]. By analogy with the stopping in cold matter [13], its accuracy can be evaluated as no worse than 1–2 % for multi-MeV protons passing through a plasma with $n_{\rm fe} \simeq 10^{19}$–$10^{20}$ cm^{-3}, where $L_{\rm fe} \simeq 10$. Strong coupling at higher matter densities is not expected to affect Eq. (1) noticeably, provided that the energy spectrum of electron excitations is quasicontinuous over the energy scale $\Delta E_e \gtrsim \hbar \omega_p$ and the density of electron states can be approximated as that of free electrons. Unfortunately, the only experiment by Belyaev *et al.* [15], where Eq. (1) was tested directly had a resolution that had not allowed to validate it any better than to an accuracy of $\pm 20\%$.

Under realistic experimental conditions, the plasma is typically only partially ionized, and its stopping power for protons is given by

$$\frac{dE_p}{dx} = -\frac{4\pi e^4 n_{\rm fe}}{m_e v_p^2} \left(L_{\rm fe} + \sum_k \frac{n_k}{n_{\rm fe}} \nu_{bk} L_{bk} \right), \tag{3}$$

where n_k is the number density of the ion species k, ν_{bk} is the number of bound electrons in the ion k, and

$$L_{bk} = \ln \frac{2 m_e v_p^2}{J_k} \tag{4}$$

is the Coulomb logarithm of the bound electrons for this species. Here J_k (eV) is the mean excitation energy (usually referred to as the mean ionization potential [13]) of the ion k.

Bound electrons introduce two additional sources of uncertainty: one associated with the ionization equilibrium (which, in particular, depends on the plasma temperature), and the other associated with the values of J_k. However, because the Coulomb logarithms L_{bk} for the bound electrons have typically a factor of 2–3 lower values than $L_{\rm fe}$, the effect of these additional uncertainties is suppressed in the case of significant ionization when the number of free electrons $n_{\rm fe}$ exceeds the total number of bound electrons $n_{\rm be} = \Sigma_k n_k \nu_{bk}$. Nevertheless, practical applications of this diagnostic method require that some information on the plasma temperature be obtained in the experiment. By using these data (for which a considerably lower level of accuracy can be tolerated) together with the measured proton energy losses, a good-quality estimate of the free electron density can be obtained.

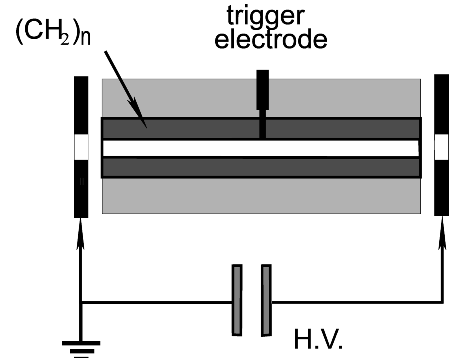

FIG. 1. Principal scheme of the plasma target.

To check the sensitivity of the inferred values of $n_{\rm fe}$ to the ionization equilibrium, we performed a series of simulations with the thermodynamic code SAHA-4, designed for computing ionization equilibria in multicomponent weakly coupled plasmas [16,17]. It should be noted here that, when calculating the ionization equilibrium, there also arises an uncertainty associated with the cutoff of the partition functions of ions, and with a modeling of the interparticle interactions. We checked the sensitivity to these effects by trying different cutoff procedures and different models for the plasma coupling. It was found that the ensuing variations in the $n_{\rm fe}$ values remained within $\pm 5\%$ for our experimental conditions.

III. EXPERIMENT

The plasma was generated by igniting an electric discharge inside an $l=50$ mm long cylindrical capillary channel bored in a polyethylene slab, as is shown schematically in Fig. 1. Two different diameters of the capillary channel have been used in the experiments, namely, $\phi=1.5$ and 3 mm. The power was supplied by a capacitor bank with a maximum stored energy of up to 150 J, and triggered by a spark-gap switch. The electrodes at both ends of the capillary have been manufactured from carbon.

The temporal history of the discharge current measured by the Rogowsky coil is shown in Fig. 2. This figure shows also the pressure of the plasma during the discharge phase for the diameter $\phi=1.5$ mm of the capillary channel. The temperature was determined by measuring the intensity of the plasma emission in the continuum spectrum in the wavelength range from 200 to 300 nm, with a reference to the standard impulse light source with a brightness temperature of 40 000 K [21]. The pressure was determined by a piezocrystal detector, which was calibrated to an accuracy of better than $\pm 10\%$.

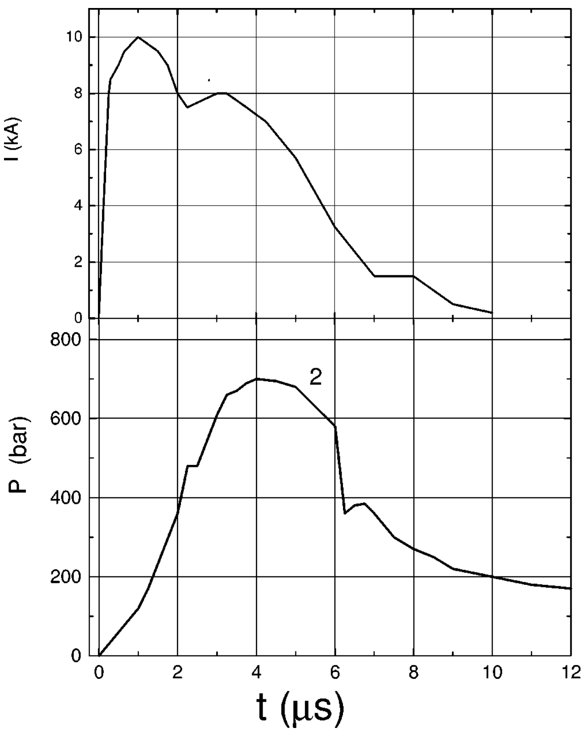

FIG. 2. Temporal evolution of the discharge current (curve 1) and plasma pressure (curve 2) in the capillary.

In our experiment we used 7-μs-long pulses of 3-MeV protons delivered by the 148.5-MHz ''Istra-36'' radio frequency quadrupolar linac at Institute for Theoretical and Experimental Physics [22]. The proton beam with a longitudinal momentum spread of $\Delta p/p = 10^{-2}$ was transported through a magnetic separator, which reduced the momentum spread down to 10^{-3}. The beam current was at a level of 1 mA after the slit of the separator magnet. As shown in Fig. 3, the plasma target was integrated into the vacuum system of the beam line. Differential pumping proved to be sufficiently effective in insulating the beam line vacuum from the pressurized target during its operation cycle. The proton energy losses were analyzed by using a dipole magnet with a deflection angle of 48° over a radius of 707 mm.

The image of the proton beam in the plane perpendicular to the beam axis was registered by using a microchannel analyzer (MCA). It consists of a microchannel plate (MCP) of a $70\times 90\text{-mm}^2$ size and a blue-light phosphoric screen mounted on a fiber optics disk. A pulsed power supply for the MCP enabled us to measure the energy of protons with a time resolution of better than 0.5 μs. The spot image of the proton beam on the screen of the microchannel analyzer was tracked by a charged-coupled-device (CCD) camera. The dependence of the image position on the strength of the magnetic field was measured by using 3-MeV protons, and then the dependence of this position on the proton energy was calculated. The proton energy loss $E_{p0}-E_{p1}$ was determined by measuring the displacement of the beam image on the screen of the microchannel analyzer.

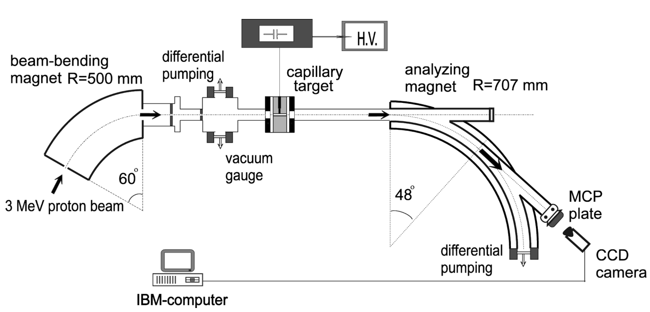

FIG. 3. Experimental setup for measuring the energy loss of 3-MeV protons in a capillary discharge.

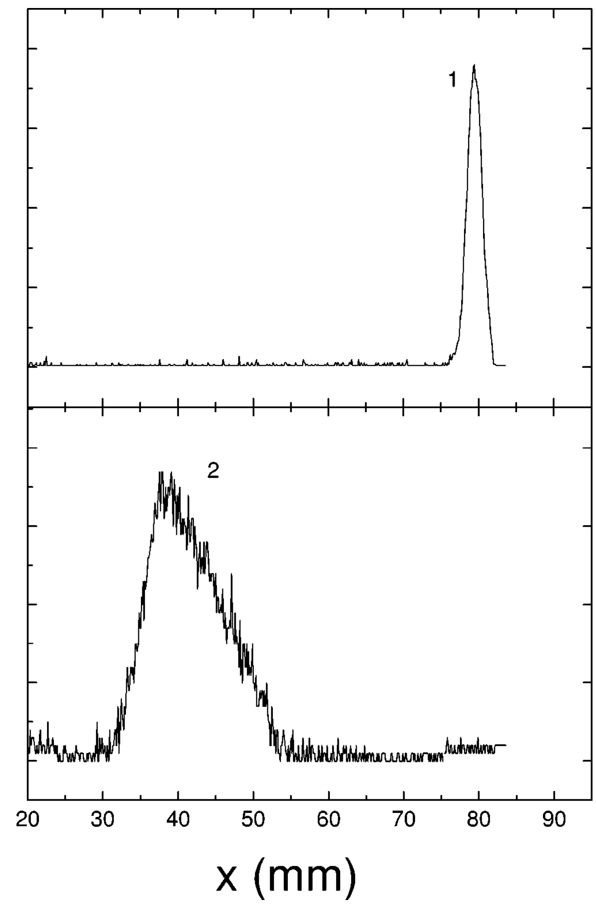

FIG. 4. Image profile of the proton beam on the MCA screen before (curve 1, $E_p = 3$ MeV) and after (curve 2, $E_p = 2.51$ MeV) ignition of the discharge.

Figure 4 shows the profiles of the beam image in the registration plane before and after the discharge was ignited. An additional time delay between the plasma ignition and the triggering of the MCP power supply allowed us to scan the proton energy losses over the operation cycle of the plasma target. The maximum energy loss by 3-MeV protons was 170 ± 79 keV for the $\phi = 3$ mm capillary, and 490 ± 75 keV for the $\phi = 1.5$ mm capillary.

IV. RESULTS

The plasma probed in our experiment was an atom-ionic mixture of initial composition CH_2 heated to a temperature $T_e \gtrsim 3.0$ eV. Having measured the energy lost by protons in the plasma column, the number density of the free electrons $n_{\rm fe}$ can be determined from Eq. (2) by replacing $L_{\rm fe}$ with the total effective Coulomb logarithm

$$L = \ln\frac{2m_e v_p^2}{\hbar\omega_p} + 6\xi_C \ln\frac{2m_e v_p^2}{J_C} + 5\xi_{C+}\ln\frac{2m_e v_p^2}{J_{C+}} + \cdots + \xi_{C+5}\ln\frac{2m_e v_p^2}{J_{C+5}} + \xi_H \ln\frac{2m_e v_p^2}{J_H}, \tag{5}$$

where $\xi_k = n_k/n_{\rm fe}$ is the ratio between the number density of the ion (atom) species k and that of the free electrons. The values of ξ_k have been calculated with the code SAHA-4 [16,17].

The mean excitation energy of atomic hydrogen, $J_H = 15.0$ eV, is well known [18]. For neutral carbon we can take the recommended experimental value $J_C = 75$ eV from Table VI in Ref. [13]. To evaluate the unknown quantities $J_{C+}, J_{C+2}, \ldots$ for a singly charged and higher carbon ions, we employ the approximate procedure proposed in Ref. [19].

For each electronic subshell j of an ion k the mean excitation energy is written as $J_{k,j} = g\epsilon_{k,j}$, where $\epsilon_{k,j}$ is the electron binding energy in this subshell, and g is an empirical factor whose values typically fall in the range $1.1 \leqslant g \lesssim 2$ (for atomic hydrogen $g = 1.105$). We assume for simplicity that g has the same value for all subshells of a given ion k, and evaluate J_k by summing up the contributions of all the populated subshells

$$J_k = g\ \exp\left(\sum_j \nu_{bk,j}\ln\epsilon_{k,j} \Bigg/ \sum_j \nu_{bk,j}\right). \tag{6}$$

Here $\nu_{bk,j}$ is the number of bound electrons in the subshell j. For neutral carbon, the value of $J_C = 75$ eV implies $g = 1.9$. Making use of the known ionization potentials for successive ions and the subshell binding energies $\epsilon_{0,j}$ of a neutral atom, we can evaluate the subshell binding energies of successive ions as [20]

$$\epsilon_{k,j} = \epsilon_{0,j} + \Delta\epsilon_k, \tag{7}$$

where $\Delta\epsilon_k$ is the difference between the ionization potential (i.e., the binding energy of the outer electron) of the ion k and the binding energy of the same electron in the neutral atom. In this way, having assumed $g = 1.5$, we calculate

$$J_{C+} \approx 115\ \text{eV}, \quad J_{C+2} \approx 190\ \text{eV}, \quad J_{C+3} \approx 300\ \text{eV} \tag{8}$$

for the ionization stages $+1 \rightarrow +3$ of carbon. The uncertainty in thus evaluated values of $\ln J_k$ can be tentatively estimated as ± 0.3, which implies some $\pm 3\%$ uncertainty for the inferred values of $n_{\rm fe}$ under our experimental conditions.

The dependence of the total effective Coulomb logarithm L on the plasma temperature T_e is illustrated in Fig. 5. The calculations have been performed for a fixed value of the plasma pressure $P = 700$ bar with the SAHA-4 code. It is seen that the free electron contribution $L_{\rm fe} = \ln(2m_e v_p^2/\hbar\omega_p) \approx 10$ is practically independent of T_e. Over the temperature range $T_e = 3.0$–3.6 eV measured in our experiment, the variation of L is due primarily to a variable contribution of C^+ ions. We estimate that the corresponding uncertainty in the value of L is no more than $\pm 8\%$.

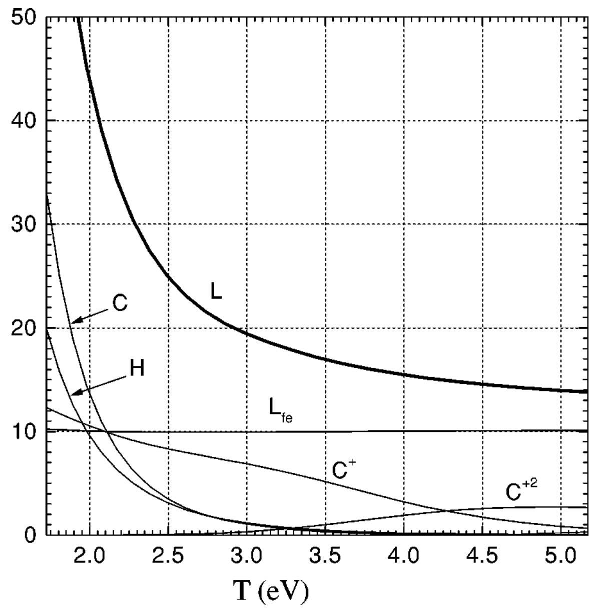

FIG. 5. Total effective Coulomb logarithm L defined by Eq. (5) and calculated as a function of plasma temperature T_e for a fixed value of pressure $P = 700$ bar. Also shown are partial contributions due to the free ($L_{\rm fe}$) and bound electrons of different ion species.

As already mentioned above, we conducted experiments for two values of the capillary diameter, $\phi = 1.5$ and 3 mm. The plasma parameters were quite stable and reproducable from shot to shot. Two quantities characterizing the plasma state were measured simultaneously, namely, the electron temperature T_e and the total plasma pressure P. The results obtained in the shots where the highest values of the proton energy loss were measured are summarized in Table I.

From Eq. (5) it is clear that, in order to infer the $n_{\rm fe}$ value by applying Eq. (2) to the measured proton energy loss, it is sufficient to have the data for only one thermodynamic quantity—either T_e or P. The results presented in Table I have been obtained by using the measured values of temperature T_e. The pressure values that were calculated with the SAHA-4 code for these $n_{\rm fe}$ and T_e agree well with the measured P values listed in Table I, which validates the overall consistency of our approach.

V. CONCLUSION

We have demonstrated that the Coulomb energy losses by fast protons can be used as a practical diagnostic method to measure the density of free electrons in plasmas. In the case

TABLE I. Summary of the experimental results.

	$E_{p0}-E_{p1}$	T_e	P	$n_{\rm fe}(T_e)$
$\phi = 1.5$ mm	490 ± 75 keV	3.3 ± 0.3 eV	700 ± 70 bar	$(6.4 \pm 1.1) \times 10^{19}$ cm^{-3}
$\phi = 3.0$ mm	170 ± 79 keV	3.3 ± 0.3 eV	250 ± 25 bar	$(2.5 \pm 1.1) \times 10^{19}$ cm^{-3}

of partially ionized plasmas, the energy loss data must be supplemented by simultaneous measurements of either the electron temperature T_e or pressure P of the probed plasma. In our experiment with the CH_2 plasma at $T_e \approx 3.3$ eV in a capillary discharge, we have been able to measure the free electron density as high as $n_{fe} = 6.4 \times 10^{19}$ cm^{-3} to an accuracy of $\pm 17\%$. The dominant contribution to the error originates from the measurement of the proton energy loss $E_{p0} - E_{p1}$.

A simple analysis (see Fig. 5) shows that the accuracy of this method should increase dramatically with the increasing plasma temperature, as more and more of the atomic electrons become excited into the continuum. In our example of the CH_2 plasma, for instance, it would simply suffice to verify that the electron temperature $T_e \gtrsim 5$ eV to be able to measure the n_{fe} values to an accuracy of about $\pm 5\%$, provided that the error for the proton energy loss is below this level.

ACKNOWLEDGMENTS

This work was supported by the INTAS Grant No. 94-1638, by the Russian Basic Research Foundation (RFBR) Grant No. 96-02-19649, and ISTC Grant No. 154. We wish to thank S. Savin, V. Turtikov, Yu. Orlov, A. Kozlov, and Yu. Stasevich for their efficient help in this work.

[1] D. Keefe, Annu. Rev. Nucl. Part. Sci. **32**, 391 (1982).

[2] R. Bock, I. Hofmann, and R. Arnold, Nucl. Sci. Appl. **2**, 97 (1984).

[3] D. H. H. Hoffmann, K. Weyrich, H. Wahl, Th. Peter, J. Meyer-ter-Vehn, J. Jacoby, R. Rimbot, D. Gardes, M. F. Rivet, M. Dumail, C. Fleurier, A. Sanba, C. Deutsch, G. Maynard, R. Noll, R. Haas, R. Arnold, and S. Maurmann, Z. Phys. A **330**, 339 (1988).

[4] C. Deutsch, G. Maynard, R. Bimbot, D. Gardes, S. Della-Negra, M. Dumail, B. Kubica, A. Richard, C. Fleurier, A. Sanba, D. H. H. Hoffmann, K. Weyrich, and H. Wahl, Nucl. Instrum. Methods Phys. Res. A **278**, 38 (1989).

[5] D. H. H. Hoffmann, K. Weyrich, H. Wahl, D. Gardes, R. Bimbot, and C. Fleurier, Phys. Rev. A **42**, 2313 (1990).

[6] K.-G. Dietrich, K. Mahrt-Olt, J. Jacoby, E. Boggasch, M. Winkler, B. Heimrich, and D. H. H. Hoffmann, Laser Part. Beams **8**, 583 (1990).

[7] F. C. Young, D. Mosher, T. A. Mehlhorn, S. J. Stephanakis, and S. A. Goldstein, Phys. Rev. Lett. **49**, 549 (1982).

[8] H. Kunze, R. Noll, C. R. Haas, M. Elfers, and J. Hertzberg, Laser Part. Beams **8**, 595 (1990).

[9] A. Golubev, G. Belyaev, M. Basko, B. Sharkov, A. Cherkasov, and A. Fertman, Fusion Eng. Des. **32-33**, 557 (1996).

[10] K. Weyrich, Ph.D. dissertation, University Heidelberg, 1988, GSI Report No. 89-5, 1989 (unpublished).

[11] N. G. Basov, Yu. A. Zakharenkov, A. A. Rupasov, G. V. Sklizkov, and A. S. Shikanov, *Dense Plasma Diagnostics* (Nauka, Moscow, 1989).

[12] C. A. Morgan, H. R. Griem, and R. C. Elton, Phys. Rev. E **49**, 3 (1994).

[13] S. P. Ahlen, Rev. Mod. Phys. **52**, 121 (1980).

[14] A. I. Larkin, Zh. Eksp. Teor. Fiz. **37**, 264 (1959) [Sov. Phys. JETP **37**, 186 (1960)].

[15] G. Belyaev, M. Basko, A. Cherkasov, A. Golubev, A. Fertman, I. Roudskoy, S. Savin, B. Sharkov, V. Turtikov, A. Arzumanov, A. Borisenko, I. Gorlachev, S. Lysukhin, D. H. H. Hoffmann, and A. T. Tauschwitz, Phys. Rev. E **53**, 2701 (1996).

[16] V. K. Gryaznov, *et al.*, Thermophysical Properties of Working Media of Gas-Phase Nuclear Reactor (Atomizdat, Moscow, 1980).

[17] W. Ebeling, A. Foerster, V. Fortov, V. Gryaznov, and A. Polishchuk, *Thermophysical Properties of Hot Dense Plasmas* (Teubner, Stuttgart-Leipzig, 1991).

[18] H. A. Bethe, Ann. Phys. (Leipzig) **5**, 325 (1930).

[19] M. M. Basko, Sov. J. Plasma Phys. **10**, 689 (1984).

[20] T. A. Carlson, C. W. Nestor Jr., N. Wasserman, and J. D. McDowell, At. Data **2**, 63 (1970).

[21] I. V. Podmoshenskii, A. M. Pukhov, and A. V. Yakovleava, Zh. Prikl. Spektrosk. **XVI**, 415 (1972) (in Russian).

[22] I. V. Chuvilo, M. M. Katz, A. M. Kozodaev, A. A. Kolomiets, N. V. Lazarev, V. K. Plotnikov, G. G. Shimchuk, O. V. Shwedov, and V. V. Vasiliev, in *Proceedings of the Fifth European Particle Accelerator Conference (EPAC96), Barcelona, 1996* (Institute of Physics, Bristol, 1996), Vol. 3, pp. 2674-2676.